Title	Enhancement of adhesion strength and cellular stiffness of osteoblasts on mirror-polished titanium surface by UV-photofunctionalization
Author(s) Alternative	Yamada, M; Miyauchi, T; Yamamoto, A; Iwasa, F; Takeuchi, M; Anpo, M; Sakurai, K; Baba, K; Ogawa, T
Journal	Acta biomaterialia, 6(12): 4578-4588
URL	http://hdl.handle.net/10130/2101
Right	

Acta Biomater

Enhancement of adhesion strength and cellular stiffness of osteoblasts on mirror-polished titanium surface by UV-photofunctionalization

Masahiro Yamada[1,2]*, Tomohiko Miyauchi[3], Akiko Yamamoto[4,5], Fuminori Iwasa[1,3], Masato Takeuchi[6], Masakazu Anpo[6], Kaoru Sakurai[2], Kazuyoshi Baba[3], and Takahiro Ogawa[1]

[1]Laboratory for Bone and Implant Sciences (LBIS), The Jane and Jerry Weintraub Center for Reconstructive Biotechnology, Division of Advanced Prosthodontics, Biomaterials and Hospital Dentistry, UCLA School of Dentistry, Los Angeles, California, USA.

[2] Department of Removable Prosthodontics & Gerodontology, Tokyo Dental College, Chiba, Japan

[3]Department of Prosthodontics, School of Dentistry, Showa University, Tokyo, Japan

[4]International Center for Materials Nanoarchitectonics, National Institute for Materials Science (NIMS), Tsukuba, Japan

[5]Biomaterials Center, National Institute for Materials Science (NIMS), Tsukuba, Japan

[6]Department of Applied Chemistry, Graduate School of Engineering, Osaka Prefecture University, Sakai, Japan

Short title: Toughened osteoblast adhesion on photofunctionalized titanium

First and second authors contributed equally.

This work was supported by Japan Medical Materials (JMM) Corporation.
All authors have no conflicts of interest.

*Corresponding author. Tel.; (+81) 043-270-3933; Fax; (+81) 043-270-3935

E-mail: masayamada@tdc.ac.jp

Acta Biomater

Abstract

Ultraviolet (UV)-photofunctionalization of titanium substantially enhances the strength and quality of osseointegration by promoting osteogenic cellular attachment and proliferation. However, the mechanism underlying the initial interaction between the cells and the surface of the material remains to be elucidated, especially where the influence of surface roughness is excluded as a factor. We evaluated the effect of UV-photofunctionalization on the adhesive strength and cellular stiffness of a single osteoblast and its association with extent of cell spread, cytoskeletal development and focal adhesion assembly on a very smooth titanium surface. Rat bone marrow-derived osteoblasts were cultured on UV-treated or -untreated mirror-polished titanium disks. The mean critical shear force required to initiate detachment of a single osteoblast (n = 10) was over 2000 nN on a UV-treated surface at 3 hr incubation, which was 17 times greater than that on an untreated surface. The mean total energy required to complete the detachment of osteoblasts (n = 10) was consistently over 60 pJ on a UV-treated titanium surface after 24 hr culture, which was up to 42 times greater than that on an untreated surface. Cellular shear modulus, which represents cellular stiffness, was consistently greater on a UV-treated surface than on an untreated surface after 24 hr incubation (n = 10). This strengthening of cell adhesion and cellular mechanical properties on UV-treated titanium was accompanied by enhanced cell spread and actin fiber development and increased levels of vinculin expression. These results indicate that UV-photofunctionalization substantially strengthens osteoblast retention on titanium bulk material with no topographical features and that this is associated with enhancement of intracellular structural development during the cell adhesion process.

Key words: bone-titanium integration; cytoskeleton; osseointegration; shear test; ultraviolet; vinculin

Introduction

Retention of osteogenic cells on the surface of a material is essential in establishing bone-material integration, and especially so for the osseointegration of implants and other such load-bearing bone anchorage devices. The implant surface needs to recruit as many osteogenic cells as possible from the local tissue [1, 2]. Cells attached to the implant surface must be capable of withstanding external forces, or cell detachment will take place. These may include compressive, tensile, or shear forces due to weight, gravity, tissue shrinkage, muscular function, flow of blood and tissue fluid, or micro-motion of the material itself [3]. The resistance of cells on a scaffold to these forces is largely dependent on the mechanical properties of the cell body [4] and cell adhesion strength [3, 5]. This is critical, as subsequent biological cascade, including proliferation, extracellular matrix (ECM) production and matrix mineralization, is regulated during the cell adhesion process by cell adhesion molecules and their signaling pathways [5-9]. The surface characteristics of the material, including topography and physicochemical properties, influence cell adhesion during the initial cell-to-material interaction [10, 11].

Recently, ultraviolet (UV)-photofunctionalization of titanium has been developed [12]. These functionalized titanium surfaces show markedly enhanced osteoconductivity, resulting in improved osseointegration capabilities. In the osseointegration of a UV-treated implant, biomechanical strength was increased 3-fold at the early healing stage and remained significantly higher, even at the late healing stage, in comparison with that in untreated implants in an animal model [12]. This substantial enhancement of osseointegration strength in UV-treated implants is supported by histological and histomorphometrical findings: almost 100% bone-implant contact was acquired around UV-treated implants as opposed to less than 55% around untreated implants [12]. In addition, it was demonstrated that UV-treated titanium implants accelerated and enhanced bone healing around implants in a periimplant cortical gap model [13].

The biological mechanism underlying this enhanced osteoconductivity in titanium by UV-photofunctionalization has been investigated. It was found that UV-treated titanium surfaces promoted cell migration, attachment and proliferation in osteoblastic cultures [12, 14]. On UV-treated titanium, osteoblastic gene expression was also up-regulated and accelerated, but not as much as cell attachment and proliferation [12, 14]. It was also shown that the *in vitro* expression of the osteoblastic phenotype was enhanced on UV-treated titanium, as evidenced by a marked increase in alkaline phosphatase activity and mineralized ECM formation compared to that on untreated titanium [12, 15]. Moreover, UV-photofunctionalization not only improves the osteoblastic affinity of titanium, but also activates and amplifies cell-to-cell interaction between different types of osteogenic cells such as bone marrow cells and periosteal cells [13]. Thus, it has been confirmed, both at the cellular and tissue levels, that UV-photofunctionalization upgrades the osseointegration capacity of titanium to a near maximum, with no need for any complex titanium surface modification such as nanotopographical or chemical modification.

A number of intriguing questions, however, remain with regard to the initial osteoblast-to-surface interactive phenomena underlying the biological effects of UV-treatment of titanium surfaces. Our previous culture study demonstrated that osteoblast adhesion is accelerated and enhanced on UV-treated titanium surfaces, as evidenced by markedly expedited cell spread, dense actin fiber formation and up-regulated expression of vinculin [16], which functions as a key membrane-cytoskeletal protein in focal adhesion plaques and is involved in linkage of integrin adhesion molecules to the actin cytoskeleton [17, 18]. A fully developed focal contact-cytoskeleton complex and advanced cell spread behavior suggest that UV-treated titanium surfaces substantially enhance osteoblastic retention. Osteoblastic culture on UV-treated titanium surface significantly resists vibratory and enzymatical detachment force [16]. Observation of cell morphology can only provide indirect evidence of enhanced osteoblastic adhesion strength on UV-treated titanium surfaces. Moreover, we cannot determine whether a detachment force is uniformly applied to all the cells in a

culture or the magnitude of cell adhesion strength to a material surface from vibratory or enzymatical approaches to evaluation such as fluid flow [19, 20] or spinning methods [21-23]. It is necessary to achieve a quantitative understanding of cell retention in order to clarify the biological mechanism underlying the bio-activation of titanium by UV-photofunctionalization and signal transduction between cells and UV-treated surfaces. Therefore, it is essential to measure direct indicators of retention such as the critical force and total energy required to achieve complete cell detachment and determine cellular mechanical properties on UV-treated titanium surfaces. We previously developed a shear test device to evaluate single-cell detachment force [24, 25]. The advantage of this device is that, unlike other detachment assay protocols, it allows us to obtain direct and absolute values for the shear force required to detach a single cell from a material surface and achieve *in situ* measurement in culture medium with none of the degenerative effects on cells involved in drying or fixation, for example [26]. In addition, the cellular shear modulus, a representative parameter of cellular stiffness, can be calculated on the basis of data obtained in this detachment assay.

Another question is whether UV treatment can induce bio-activation of titanium even on an absolutely smooth surface with no roughness or topographic features such as one that has been mirror-polished. The topographic and physicochemical properties of a substrate's surface determine and coordinate cell spread and adhesion strength. To our knowledge, all previous studies on UV-mediated biological enhancement have used titanium bulk with either machined, acid-etched or sand-blasted surfaces whose average roughness values were 100-600 nm [12, 15]. Such surface roughness *per se* facilitates osteoblastic differentiation, but then delays and limits cell spread [12, 14]. Essentially, cells tend to spread more extensively on a smoother and/or more hydrophilic surface. However, an absolutely smooth and hydrophilic surface is generally poor in cell retention property, which is unfavorable in terms of tissue integration. This principle underlies cell sheet technology using polymer poly(N-isopropylacrylamide) plates that convert hydrophobic surfaces to hydrophilic surfaces in response to temperature [27-29]. UV-photofunctionalization results in the wettability of

titanium surfaces, converting them from hydrophobic to hydrophilic [12, 14, 15]. Therefore, to evaluate the universality of the biological benefits of UV-photofunctionalization in terms of the osseointegration of implants and other such bone anchorage devices, it is necessary to determine whether UV-treatment enhances osoteoblastic adhesion to titanium surfaces regardless of surface topography.

To clarify these two questions, the purposes of this culture study were to measure osteoblastic retention capability in terms of critical shear force, total detachment energy and cellular elastic modulus on mirror-polished titanium surfaces with or without UV-pretreatment using single-cell detachment technology and determine the extent of cell spread, cytoskeletal development and focal adhesion assembly.

Materials and methods

Titanium samples and surface characterization

Commercially available, pure, grade-2 titanium disks, 20 mm in diameter, were polished with a grinding machine with a graded series of sandpapers and a buff. Polished titanium disks were rinsed with a graded series of ethanol and finally washing with distilled water in an ultrasonic machine. The surface morphology of the titanium disks was examined using a laser microscope (VK-8700, Keyence, Osaka, Japan). The average roughness (Ra), peak-to-valley roughness (Ry) and inter irregularities space (Sm) were calculated.

Titanium disks were stored after polishing and washing under dark ambient sterile conditions for 4 weeks according to a protocol established previously [13, 15]. Half of the titanium samples were then treated with UV light for 48 hr under ambient conditions using a 15W bactericidal lamp (Toshiba, Tokyo, Japan); intensity: ca. 0.1 mW/cm^2 ($\lambda = 360 \pm 20$ nm) and 2 mW/cm^2 ($\lambda = 250 \pm 20$ nm) using a previously established protocol [12, 13, 15]. To verify the effect of UV treatment, the

chemical composition of the titanium surfaces was evaluated by electron spectroscopy for chemical analysis (ESCA) before and after UV treatment. ESCA was performed by X-ray photoelectron spectroscopy (XPS) (ESCA3200, Shimadzu, Tokyo, Japan) under high vacuum conditions (6×10^{-7} Pa). The wettability of the titanium samples surfaces at before and after UV treatment was measured as the contact angle of a 10-μl H_2O droplet.

Osteoblast cell culture

Bone marrow cells isolated from the femurs of 8-week-old, male, Sprague-Dawley rats were grown in alpha-modified Eagle's medium supplemented with 15% fetal bovine serum, 50 μg/ml ascorbic acid, 10 mM Na-β-glycerophosphate, 10^{-8}M dexamethasone and antibiotic-antimycotic solution according to a previously established method [30]. Cells were incubated in a humidified atmosphere of 95% air and 5% CO_2 at 37°C. When 80% confluent, the cells were detached using 0.25% trypsin-1mM EDTA-4Na and seeded onto substrates at a density of 3×10^4 cells/cm^2. The culture medium was renewed every 3 days. This study protocol was approved by the University of California at Los Angeles Chancellor's Animal Research Committee.

Measurement of attached cell number

Initial attachment of cells was evaluated by measuring the amount of cells attached to the substrates at after 3 or 24 hr incubation. These quantifications were performed using WST-1-based colorimetry (WST-1, Roche Applied Science, Mannheim, Germany). The culture well was incubated at 37°C for 4 hr with 100 μl tetrazolium salt (WST-1) reagent. The amount of formazan product was determined using an ELISA plate reader (Synergy HT, BioTek Instruments, Winooski, VT) at 420 nm.

Single-cell detachment technique

To evaluate strength of osteoblastic adhesion to the substrate surfaces, shear force and total energy

required to detach a single osteoblast were measured. This technique was developed and established as a useful measure to quantify the adhesion strength of various cell types adhering to various biomaterial surfaces with or without an ECM coating. The details of this procedure are described elsewhere [24, 25]. Osteoblastic cells cultured for 3, 8 or 24 hr were subjected to detachment by horizontal shear force. The culture dish was placed on the computer-controlled XY-stage of the device, which was monitored under phase-contrast microscopy. While the cells were continuously incubated in the culture medium, the tip of the cantilever pushing head approached a single cell at an approximately 90 degree angle to the long axis of the cell at its middle (Fig. 1A). The distance between the pointed head of the tip and the surface of the titanium substrate was kept to approximately 0.2 μm throughout all measurements. While a horizontal pushing force was applied at a speed of 20 μm/s, a force-displacement curve was obtained (Fig. 1A). Point A in a force-displacement curve (Fig. 1A) is where the tip of the cantilever makes initial contact with the single cell; Point B is where the magnitude of the pushing force reaches its peak, and is assumed to be the moment when cell detachment is initiated. Subsequently, the force applied decreases until complete detachment of the cell is attained (Point C). The force at Point B is defined as the critical shear force; the area A-B-C-A is supposed to correspond to the total energy required to completely detach a single cell and is, therefore, defined as the total detachment energy.

Evaluation of cellular mechanical properties

To evaluate the mechanical properties of the osteoblast on the titanium surface, we assumed that the cell was an isotropic and linear elastic solid. We then calculated the shear modulus, a typical stiffness parameter of cellular bodies, from the stress and strain applied to the cell in the single-cell detachment assay on the basis of Hooke's Law [31]. Hooke's law can be applied to linear elastic solid materials. The force-displacement curves obtained represent the interdependence of the cantilever deflection (detachment force) and relative sample position (displacement). Data obtained from the single detachment experiment were incorporated into the following Hooke's Law formula:

Shear modulus = stress/strain ($E = \sigma/\varepsilon$)

The equation for stress (σ) was as follows:

σ = Critical shear force/cell area (F/A: Pa)

After substituting the stress equation into the formula, the following equation was obtained:

$E = F/(A \times \varepsilon)$

With this equation, a greater value was obtained for the shear modulus of the osteoblast with an increase in critical shear force or decrease in cell area or cellular strain.

The formula for strain (ε) was as follows:

ε = amount of displacement (μm) between initial contact with cantilever (Point A) and point of critical shear (Point B) (distance between point A and D)/Cell width in direction of movement of cantilever tip ($\Delta L/L$) (see Fig. 1B)

Cell area (A) and cell width in direction of movement of cantilever tip (L) was measured in light microscopic live images before cell detachment. All relevant measured values were substituted into the equation for calculation of shear modulus.

Morphology and morphometry of cells

Confocal laser scanning microscopy was used to examine cell morphology and cytoskeletal arrangement

in osteoblasts. After 3 or 24 hr culture, cells were fixed in 10% formalin and stained using the fluorescent dye rhodamine phalloidin (actin filament, red color; Molecular Probes, Eugene, OR). The area, perimeter and Feret's diameter of the cells were quantified using an image analyzer (ImageJ, NIH, Bethesda, ML).

Vinculin and actin expression analysis

The expression and localization of the focal adhesion protein vinculin were analyzed by microscopic image-based observation and densitometry at 3 or 24 hr culture. During preparation for the confocal microscopic analysis, the cultures were also immunochemically stained with mouse anti-vinculin monoclonal antibody (Abcam, Cambridge, MA), followed by FITC-conjugated anti-mouse secondary antibody (Abcam). The level of vinculin expression was quantified as a pixel-based density using an image analyzer (ImageJ, NIH, Bethesda, ML). The density was calculated in two ways: cell-based expression (total pixels/cell number) and cell area-based expression (total pixels/total cell area). Densitometry was also applied to quantify the expression of actin filaments in the same manner using images stained with rhodamine phalloidin.

Statistical analysis

The number of samples was 10 for a single-cell detachment assay, cellular elastic modulus and cell morphometry. Quantification of vinculin and actin expressions was performed using 9 cells. The number of samples for the cell attachment and proliferation assays and surface characterization of titanium disks was 3. A one-way ANOVA was used to determine the effects of UV treatment; $p < 0.05$ was considered significant.

Results

UV-treatment does not change topography of mirror-polished titanium surfaces

Macroscopic images (Fig. 2A) revealed that the titanium surfaces used in this study were sufficiently

mirror-polished to reflect the figure of the camera's lens. High magnification laser microscopic images showed that mirror-polished titanium surfaces both with and without UV-treatment were smooth and flat, with no topographical features, roughness or differences at the micro level (Fig. 2B). Overhead contour map images reconstructed after laser scanning in a vertical scale of 20 μm showed similar surface morphologies for both surfaces, with no 3-dimensional structures at the sub-micron level (Fig. 2B). Quantitative assessment of surface roughness on the mirror-polished titanium surfaces showed that there were no significant differences between with and without UV-treatment for all parameters tested (Ra, Ry, Sm) (Fig. 2C).

UV-treatment changes physicochemical properties of mirror-polished titanium surfaces

The XPS profile (Fig. 2D) showed a reduction in the intensity/cps values of carbon atoms (C1s) and an increase in that of oxygen and titanium atoms on mirror-polished titanium surfaces with UV-treatment. The atomic percentage of carbon on mirror-polished titanium surfaces was reduced by over 50% to less than 20% after UV-treatment. Accordingly, the percentage of titanium and oxygen increased on UV-treated mirror-polished titanium surfaces (Fig. 2D). Mirror-polished titanium surfaces were hydrophobic (contact angle of H_2O > 70°) and changed to super-hydrophilic after UV-treatment (contact angle < 5°) (Fig. 2E), as shown in side views of a 10-μl H_2O dropped onto the titanium disk. Top views showed that the H_2O droplet spread more over UV-treated surfaces, while it remained in a rounded form on untreated surfaces. The percentage of H_2O spread area was almost 100% on UV-treated titanium surfaces, while it was under 5% on untreated surfaces (Fig. 2E).

UV-treatment increases number of attached osteoblasts on mirror-polished titanium surfaces

The number of attached osteoblasts was 1.4 times greater on UV-treated surfaces than on untreated surfaces at after 3 hr incubation (Fig. 3). Even at after 24 hr incubation, UV-treated surfaces had a 1.8-times greater number of attached osteoblasts than untreated surfaces.

UV-treatment enhances spreading of osteoblasts on mirror-polished titanium surfaces

Confocal laser microscopic images after actin staining with rhodamine phalloidin revealed that osteoblast spread was markedly greater on UV-treated titanium than on untreated titanium at after 3 hr incubation (Fig. 4A). Expanded osteoblasts with extended cellular processes were seen on UV-treated titanium surfaces, while large numbers of cells were still in a rounded form at this time point. At 24 hr after seeding, the cells were larger than those at 3 hr on both surfaces. However, the cells were larger on UV-treated surfaces than on untreated surfaces, even at this time of culture. The cells on UV-treated surfaces consistently showed significantly higher values than those on untreated surfaces for cytomorphometric parameters (cell area, perimeter and Feret's diameter) at 3 and 24 hr (Fig. 4B).

UV-treatment enhances actin fiber formation in osteoblasts on mirror-polished titanium surfaces

Confocal laser microscopic images after actin staining (Fig. 4A) revealed the presence of many, well-arranged actin fibers in the cytoplasm (white arrowheads in Fig. 4A) of the osteoblasts on UV-treated titanium surfaces in contrast with little actin fiber formation in osteoblasts on untreated surfaces. At after 24 hr incubation, osteoblasts on untreated surfaces showed formation of actin fibers. However, this development was inferior to that in osteoblasts cultured on UV-treated surfaces, which was extensive, dense and intensive. Image-based morphometric quantification for actin fiber formation revealed that the extent of actin fiber expression in an individual osteoblast was markedly higher on UV-treated surfaces than on untreated surfaces at both 3 and 24 hr incubation (12 and 4 times higher at 3 and 24 hr, respectively) (Fig. 4C). Density of actin fiber formation in an individual osteoblast, that is, the extent of actin fiber expression divided by cell area, was also markedly higher on UV-treated surfaces than on untreated surfaces at both 3 and 24 hr incubation (9 and 3 times higher at 3 and 24 hr, respectively).

UV-treatment enhanced the extent but not the density of vinculin expression in osteoblasts on mirror-polished titanium surfaces.

UV-treatment enhances speed and spatial extent, but not terminal density, of vinculin expression in osteoblasts on mirror-polished titanium surfaces

Confocal laser microscopic images after anti-vinculin antibody staining (Fig. 4A) overlaid with images of actin expression showed that osteoblasts on both surfaces expressed vinculin in their cytoplasm at 3 hr incubation. However, vinculin expression concentrated at the tip of cellular projections was seen only on UV-treated surfaces at this incubation-time point (white headings in Fig. 4A). At after 24 hr incubation, vinculin expression in osteoblasts cultured on untreated surfaces was not only extensively distributed within the cytoplasm, but also localized at the tip of the cytoplasmic projections. Osteoblasts cultured on UV-treated surfaces for 24 hr extensively and intensively expressed vinculin within their well-spread cytoplasms and at their extended cellular projections. Image-based morphometric quantification revealed that the extent of vinculin expression in an individual osteoblast was substantially higher on UV-treated surfaces than on untreated surfaces at both 3 and 24 hr incubation (8.3 and 1.8 times higher at 3 and 24 hr, respectively) (Fig. 4D). Density of vinculin expression in an individual osteoblast, that is, the extent of vinculin expression divided by cell area was 8 times higher on UV-treated surfaces than on untreated surfaces at 3 hr after seeding. However, the value at 24 hr incubation showed no significant difference between on UV-treated and untreated surfaces.

UV-treatment enhances individual osteoblast adhesion strength on mirror-polished titanium surfaces

The critical shear force and total detachment energy of a single osteoblast on titanium were measured by a single detachment technique. At 3 hr incubation, the mean critical shear force required to initiate detachment of a single osteoblast was 2092 ± 200 nN on UV-treated surfaces, which was 17 times

greater than that on untreated surfaces (121 ± 40 nN) (Fig. 5A). The force on UV-treated surfaces remained at the same level even at 8 hr incubation (2266 ± 860 nN), which was significantly greater than that on untreated surfaces (1324 ± 450 nN). The force on UV-treated surfaces tended to be higher than that on untreated surfaces at 24 hr incubation, but not significantly so. Osteoblasts on UV-treated titanium showed 63.7 ± 13.5 pJ in total cell detachment energy, which was 42 times greater than that on untreated surfaces at 3 hr incubation (1.5 ± 0.68 pJ) (Fig. 5B). The energy of osteoblasts on untreated surfaces markedly increased at 8 or 24 hr incubation (32.6 ± 13.4 and 26.0 ± 11.1 pJ, respectively) as compared to that at 3 hr. However, osteoblasts on UV-treated surfaces consistently showed over 60 pJ in total cell detachment energy for up to 24 hr incubation, which was consistently greater than that on untreated surfaces.

UV-treatment enhances osteoblast elastic modulus on mirror-polished titanium surfaces

Cellular elastic modulus, a representative parameter for evaluation of the mechanical properties of cellular bodies, was markedly greater on UV-treated surfaces than on untreated surfaces at all incubation time points tested (Fig. 5C). Shear modulus of osteoblasts at 3 hr incubation was 11.5 ± 4.9 kPa on UV-treated surfaces, which was 8.5 times greater than that on untreated surfaces (1.4 ± 0.6 kPa). The value for osteoblasts cultured on untreated surfaces increased by 2-3 times at 8 and 24 hr incubation (4.5 ± 1.5 and 3.3 ± 1.2 kPa, respectively) as compared to that at 3 hr. However, osteoblasts cultured on UV-treated surfaces showed 11.9 ± 4.2 and 8.7 ± 6.6 kPa at 8 and 24 hr incubation, respectively, which was a consistently 2.7-times greater value than that on untreated surfaces.

Discussion

First, we determined whether the changes in physicochemical properties and enhanced affinity for bone marrow-derived osteoblasts during the initial stages of culture induced by UV-photofunctionalization of titanium surfaces were also seen in mirror-polished titanium surfaces.

Our previous studies demonstrated an increase in the occupancy of carbon and a reduction in osteoblast attachment and protein absorption on bulk titanium surfaces over storage-time in a sterile atmosphere after surface preparation including machining and acid-etching, which was termed the "biological aging of titanium" [32-34]. This time-dependent degradation of biological activity on the titanium surface was statistically correlated with an increase in the occupancy of carbon. In addition, ultraviolet treatment of aged surfaces increased bioactivity to a level greater than that observed on freshly prepared surfaces [34]. UV-treatment resulted in a clear reduction in the atomic occupancy of carbon on the titanium surface (from over 50% to less than 20%), a proven basic premise for bio-activation by UV-photofunctionalization, together with a change from low wettablity to super-hydrophilicity. Furthermore, UV-treatment also resulted in a substantial increase in the number of attached osteoblasts during the the initial stages of culture. These results indicate that UV-treatment, which we previously developed, functionalizes titanium, regardless of surface roughness.

The quality of the polished titanium disk was evaluated by laser microscopy in this study. The observed roughness values were all extremely low although there remained minuscule variations. For example, the Ry value was approximately 200 nm (Fig. 1C), which is higher than the molecular dimensions of large proteins. However, the Ra value of culture-grade polystyrene plate is approximately 0.05 μm [35], which is higher than that of the titanium surface used in the present study (approximately 0.025 μm). This indicates that the mirror-polished titanium surfaces used in the present study could be regarded as very smooth surface, with no significant topographical features.

Enhancement of cell adhesion would lead to the prevention of cell detachment by external forces and an increase in the number of viable cells on a biomaterial under *in vivo* conditions. In addition, for anchorage-dependent cells such as osteoblasts, the degree and nature of initial attachment behavior influences their subsequent function on a scaffold [5-9]. As the confocal microscopic images in this

study show (Fig. 4), cell adhesion was promoted and enhanced on mirror-polished titanium surfaces after UV-treatment in a similar manner to that seen on roughened surfaces in our previous report [16]. In this study, osteoblasts on UV-treated titanium surfaces showed a well-elongated shape with development of cellular projections and a dense cytoskeletal structure (Fig. 4A). Moreover, actin filaments appeared earlier, were arranged well at 3 hr incubation and remained at a greater density and intensity at 24 hr incubation than those on untreated surfaces (Fig. 4A and C). These results indicate that UV-treatment not only accelerated, but also augmented the cytoskeletal development of the osteoblasts. All cell morphometric values regarding cell size and actin fiber formation on UV-treated surfaces were greater than those on untreated surfaces both at 3 and 24 hr after seeding, the initial and final stages of cell adhesion (Fig. 4B and C).

The enhanced cell spread and cytoskeletal development on UV-treated surfaces was accompanied by an increase in level of vinculin expression. Vinculin expression was not only higher, but also emerged earlier and was concentrated more at the tip of the cellular projections on UV-treated surfaces than on untreated surfaces. In addition, osteoblasts on UV-treated surfaces showed an increase in the area within an individual cell at both the beginning and the end of the cell adhesion period, but no significant increase in density-to-cell area at the end of the cell adhesion period, a result similar to that obtained in our earlier study [16]. This indicates that UV-treatment of titanium surfaces does not directly up-regulate vinculin expression in osteoblasts, but rather results in the formation of focal adhesion patches as cell spread progresses.

As described in the Material and Methods, cell detachment force and energy were determined by an analysis of the force-displacement curve obtained by detachment of a single cell from a titanium surface with a cantilever applying a lateral load to the cell at a constant velocity. A more detailed description of this device and process was reported in earlier studies [24, 25]. Point B in Figure 1A represents the first point on the bottom of the cell which became detached from the surface of the

substrate. Until point B, no disruption of cell-material binding occurred, only deformation due to the load applied with the tip of the cantilever. For this reason, maximum shear force required for cell detachment was termed “critical shear force” and degree of displacement from point A to B (⊿L) was used for calculation of cellular strain. After point B, cell detachment progresses, with disruption of each cell–material bond, one after the other. Finally, the cell becomes completely detached from the material surface at point C; all of the cell–material bonds have now been disrupted. Cell detachment energy is measured as the area of the force-displacement curve and is composed of two parts: energy for cell deformation and energy for disruption of cell–material binding. The energy supplied to the cell between points A and B (which corresponds to area A-B-D-A in Fig. 1B) is consumed mostly in deformation of the cell. Energy supplied to the cell between points B and C (which corresponds to area B-C-D-B in Fig. 1B) is consumed mainly in disruption of cell–material bonding, that is, the sum of the energy necessary to disrupt each cell–material bond.

Ultraviolet treatment enhanced adhesion strength and the cellular mechanical properties of individual osteoblasts on mirror-polished titanium surfaces. For example, the critical shear force needed to initiate cell detachment and the total detachment energy needed to complete cell detachment in an individual osteoblast was 17 times and 42 times higher on UV-treated surfaces than on untreated surfaces at 3 hr after seeding, respectively. Moreover, UV-treatment enhanced cellular shear modulus in an individual osteoblast on titanium mirror-polished surfaces by 8.5 times as compared to that on untreated surfaces. These results clearly indicate that cell retention is increased, even on mirror-polished titanium surfaces, after UV-treatment, resulting in greater resistance to shear and compressive (or tensile) forces which might cause cell detachment during the initial stages of cell adhesion.

Cellular stiffness and cell adhesion strength determine the resistance of cells on a material to detachment force [4] [3, 5]. As described above, the cellular detachment process can be split into two

phases at point B in the force-displacement curve (see figure 1A) when force is applied laterally, as in this study. No detachment, only deformation occurs until point B, which indicates the starting point of disruption of cell-material binding. Therefore, we calculated cellular shear modulus as a representative parameter of cellular stiffness by using data in the force-displacement curve from point A to B and individual cell morphometry. This calculation principle is analogous to that of the atomic force microscopic (AFM) method [31, 36], which involves substituting data acquired from a cell detachment assay into the Hooke's Law formula. This method is known to have several limitations. For example, it assumes that the cells are purely linear elastic and isotropic. However, it is more appropriate to regard cells as having a heterogeneity linked to their internal structure and surface properties. Therefore, the method used in the present study may not necessarily lead to the acquisition of absolute values. However, it should be sufficient to provide valuable information based on evaluation of relative changes or tendencies [36, 37] in the mechanical properties of an individual adherent osteoblast due to the influence of UV-treatment of titanium surfaces.

Focal adhesion complexes are specialized structures that harbor a large number of cytoskeletal proteins and one of the highest concentrations of signaling molecules in cells [38]. These multi-protein complexes are capable of capturing and integrating many signals from both the extracellular and intracellular environments [39]. Such signals transmit via cell adhesion membrane molecules, integrins, to adaptor proteins in the focal adhesion plaque, including talin and vinculin. These molecules have binding sites for actin filaments and signaling proteins, including paxillin and focal adhesion kinase (FAK) [40], which regulate formation of cellular projections and the cytoskeletal actin fiber network [41, 42]. Vinculin, in particular, has multiple binding partners. In a focal adhesion plaque, the amino-terminal in the vinculin molecule binds to talin, which, in turn, binds to β-integrins, and the carboxy-terminal binds to actin, phospholipids and paxillin-forming homodimers [43-45]. Vinculin plays a key role in initiating and establishing cell adhesion, formation of cell shape and cytoskeletal development [6, 40, 43, 46], which is indispensable for the coordinated

control of fundamental cellular processes, including differentiation, cell cycle control, apoptosis and motility [38, 46].

The mechanical properties of a cell are determined by its cytoskeleton [47, 48], which is a filamentous network composed of three types of element, including actin filaments, microtubules and intermediate filaments. Among these three elements, actin filaments are the most important, as the disruption of microtubules showed no effect on the mechanical properties of cells measured by AFM [49, 50]. Vinculin is considered to be involved in cellular shear modulus [51]. In addition to the recruitment of the cytoskeleton and vinculin, the number of bound integrin receptors and the position of adhesive patches comprising those receptors are known to regulate cell adhesion strengthening [52, 53]. The expedition and advancement of cell spread accompanying focal adhesion assembly and cytoskeletal development may contribute to the enhancement of the capability of osteoblasts to adhere to UV-treated titanium.

The point at which osteoblasts became fully detached was unclear from the results of the present study. There are a number of hypothetical detachment modes such as extracellular abruption at integrin-ECM bonds or the ECM-material surface and disruption of intracellular bonding between integrin-vinculin or vinculin-actin [24, 25]. The detachment mode is influenced by type and quality of ECM, cell type, type and number of integrin ligands and the material's surface characteristics [3, 25, 52-56]. The cell-material interactive mechanism underlying bio-activation on UV-treated titanium surfaces remains to be fully clarified. Protein absorption, including that of albumin and fibronectin, markedly increases on titanium after UV-treatment [12]. This phenomenon may be associated with the enhanced osteoblastic cell affinity observed on UV-treated titanium surfaces. In addition, a direct interaction between the cell and the UV-treated titanium surface was proposed in our previous experiment using a serum-free culture [16]. As described above, UV-treatment is known to change the physicochemical properties of the titanium surface, resulting in super-hydrophilicity

and a reduced atomic percentage of carbon. When oxygen-containing hydrocarbons covering the passive oxide film (TiO_2) on titanium surfaces [57, 58] are removed by UV-light treatment, Ti^{4+} sites are exposed, which may result in a trend toward a positive electric charge on the titanium surface. Based on the results of an earlier study, we assumed that such cationic sites on titanium accompanied by hydrocarbon decomposition, rather than super-hydrophilicity, may promote interaction with proteins and cells [12]. In fact, UV-enhanced cell adhesion was abrogated when UV-treated titanium surfaces were electrostatically neutralized by either removing the electric charge or masking with monovalent anions, while the surfaces maintained super-hydrophilicity [16]. Clarification of how interfacial signal transmission from material to cell results in osteoblastic affinity and adhesion strengthening on UV-treated titanium surfaces will be of great interest.

Titanium material is essential for bone anchorage devices, including femoral stems, orthopedic fixation screws and dental implants. Osteoblasts must adhere to titanium surfaces with various topographies depending on the device's structural and surface design. Taken together with the results of earlier studies on rough-surface titanium such as machined, acid-etched and sandblasted titanium [12-16], the present results obtained using very smooth, mirror-polished titanium surfaces indicate that UV-photofunctionalization technology can be universally applied to the bio-activation of titanium bulk material/devices, regardless of surface topography.

In conclusion, osteoblastic adhesion strength and the cellular elasticitic modulus were enhanced on UV-treated titanium with a very smooth, mirror-polished surface. To our knowledge, this is the first study to demonstrate that osteoblasts adhered to a UV-treated titanium surface are substantially more resistant to external detachment forces than those adhered to untreated titanium surfaces. This strengthening of the cellular retention capability of UV-treated surfaces was accompanied by a marked enhancement of cell spread and cytoskeletal development and increased levels of vinculin expression. The results of this study also indicate the possibility that UV-treatment is effective for

osteoblastic activation on any titanium bulk material, regardless of surface topography, showing the universal effectiveness of UV-photofunctionalization for titanium bone anchorage devices.

Acknowledgment

This work was supported by Japan Medical Materials (JMM) Corporation. The authors would like to thank Associate Professor Jeremy Williams, Tokyo Dental College, for his assistance with the English of the manuscript.

References

[1] Kuznetsov SA, Mankani MH, Gronthos S, Satomura K, Bianco P, Robey PG. Circulating skeletal stem cells. J Cell Biol 2001;153:1133.

[2] Wexler SA, Donaldson C, Denning-Kendall P, Rice C, Bradley B, Hows JM. Adult bone marrow is a rich source of human mesenchymal 'stem' cells but umbilical cord and mobilized adult blood are not. Br J Haematol 2003;121:368.

[3] Engler AJ, Chan M, Boettiger D, Schwarzbauer JE. A novel mode of cell detachment from fibrillar fibronectin matrix under shear. J Cell Sci 2009;122:1647.

[4] Lipowsky R, Sackmann E. Structure and Dynamics of Membranes. Amsterdam: North Holland, 1995.

[5] Clark EA, Brugge JS. Integrins and signal transduction pathways: the road taken. Science 1995;268:233.

[6] Buckley CD, Rainger GE, Bradfield PF, Nash GB, Simmons DL. Cell adhesion: more than just glue (review). Mol Membr Biol 1998;15:167.

[7] Mata A, Su X, Fleischman AJ, Roy S, Banks BA, Miller SK, Midura RJ. Osteoblast attachment to a textured surface in the absence of exogenous adhesion proteins. IEEE Trans Nanobioscience 2003;2:287.

[8] Wang C, Gong Y, Zhong Y, Yao Y, Su K, Wang DA. The control of anchorage-dependent cell behavior within a hydrogel/microcarrier system in an osteogenic model. Biomaterials 2009;30:2259.

[9] Grigoriou V, Shapiro IM, Cavalcanti-Adam EA, Composto RJ, Ducheyne P, Adams CS. Apoptosis and survival of osteoblast-like cells are regulated by surface attachment. J Biol Chem 2005;280:1733.

[10] Kieswetter K, Schwartz Z, Dean DD, Boyan BD. The role of implant surface characteristics in the healing of bone. Crit Rev Oral Biol Med 1996;7:329.

[11] Schwartz Z, Kieswetter K, Dean DD, Boyan BD. Underlying mechanisms at the

bone-surface interface during regeneration. J Periodontal Res 1997;32:166.
[12] Aita H, Hori N, Takeuchi M, Suzuki T, Yamada M, Anpo M, Ogawa T. The effect of ultraviolet functionalization of titanium on integration with bone. Biomaterials 2009;30:1015.
[13] Ueno T, Yamada M, Suzuki T, Minamikawa H, Sato N, Hori N, Takeuchi K, Hattori M, Ogawa T. Enhancement of bone-titanium integration profile with UV-photofunctionalized titanium in a gap healing model. Biomaterials 2009;31:1546.
[14] Aita H, Att W, Ueno T, Yamada M, Hori N, Iwasa F, Tsukimura N, Ogawa T. Ultraviolet light-mediated photofunctionalization of titanium to promote human mesenchymal stem cell migration, attachment, proliferation and differentiation. Acta Biomater 2009;5:3247.
[15] Att W, Hori N, Iwasa F, Yamada M, Ueno T, Ogawa T. The effect of UV-photofunctionalization on the time-related bioactivity of titanium and chromium-cobalt alloys. Biomaterials 2009;30:4268.
[16] Iwasa F, Hori N, Ueno T, Minamikawa H, Yamada M, Ogawa T. Enhancement of osteoblast adhesion to UV-photofunctionalized titanium via an electrostatic mechanism. Biomaterials 2010;31:2717.
[17] Puklin-Faucher E, Sheetz MP. The mechanical integrin cycle. J Cell Sci 2009;122:179.
[18] Mierke CT. The role of vinculin in the regulation of the mechanical properties of cells. Cell Biochem Biophys 2009;53:115.
[19] Truskey GA, Pirone JS. The effect of fluid shear stress upon cell adhesion to fibronectin-treated surfaces. J Biomed Mater Res 1990;24:1333.
[20] van Kooten TG, Schakenraad JM, van der Mei HC, Dekker A, Kirkpatrick CJ, Busscher HJ. Fluid shear induced endothelial cell detachment from glass--influence of adhesion time and shear stress. Med Eng Phys 1994;16:506.
[21] Boettiger D. Quantitative measurements of integrin-mediated adhesion to extracellular matrix. Methods Enzymol 2007;426:1.
[22] Garcia AJ, Ducheyne P, Boettiger D. Quantification of cell adhesion using a spinning disc device and application to surface-reactive materials. Biomaterials 1997;18:1091.
[23] Lotz MM, Burdsal CA, Erickson HP, McClay DR. Cell adhesion to fibronectin and tenascin: quantitative measurements of initial binding and subsequent strengthening response. J Cell Biol 1989;109:1795.
[24] Yamamoto A, Mishima S, Maruyama N, Sumita M. A new technique for direct measurement of the shear force necessary to detach a cell from a material. Biomaterials 1998;19:871.
[25] Yamamoto A, Mishima S, Maruyama N, Sumita M. Quantitative evaluation of cell attachment to glass, polystyrene, and fibronectin- or collagen-coated polystyrene by measurement of cell adhesive shear force and cell detachment energy. J Biomed Mater Res 2000;50:114.
[26] Nakamura H, Shim J, Butz F, Aita H, Gupta V, Ogawa T. Glycosaminoglycan degradation reduces mineralized tissue-titanium interfacial strength. J Biomed Mater Res A 2006;77:478.
[27] Yang J, Yamato M, Kohno C, Nishimoto A, Sekine H, Fukai F, Okano T. Cell sheet

engineering: recreating tissues without biodegradable scaffolds. Biomaterials 2005;26:6415.
[28] Masuda S, Shimizu T, Yamato M, Okano T. Cell sheet engineering for heart tissue repair. Adv Drug Deliv Rev 2008;60:277.
[29] Yang J, Yamato M, Shimizu T, Sekine H, Ohashi K, Kanzaki M, Ohki T, Nishida K, Okano T. Reconstruction of functional tissues with cell sheet engineering. Biomaterials 2007;28:5033.
[30] Saruwatari L, Aita H, Butz F, Nakamura HK, Ouyang J, Yang Y, Chiou WA, Ogawa T. Osteoblasts generate harder, stiffer, and more delamination-resistant mineralized tissue on titanium than on polystyrene, associated with distinct tissue micro- and ultrastructure. J Bone Miner Res 2005;20:2002.
[31] Hinterdorfer P, Dufrene YF. Detection and localization of single molecular recognition events using atomic force microscopy. Nat Methods 2006;3:347.
[32] Hori N, Ueno T, Suzuki T, Yamada M, Att W, Okada S, Ohno A, Aita H, Kimoto K, Ogawa T. Ultraviolet light treatment for the restoration of age-related degradation of titanium bioactivity. Int J Oral Maxillofac Implants;25:49.
[33] Hori N, Att W, Ueno T, Sato N, Yamada M, Saruwatari L, Suzuki T, Ogawa T. Age-dependent degradation of the protein adsorption capacity of titanium. J Dent Res 2009;88:663.
[34] Suzuki T, Hori N, Att W, Kubo K, Iwasa F, Ueno T, Maeda H, Ogawa T. Ultraviolet treatment overcomes time-related degrading bioactivity of titanium. Tissue Eng Part A 2009;15:3679.
[35] Kim MJ, Choi MU, Kim CW. Activation of phospholipase D1 by surface roughness of titanium in MG63 osteoblast-like cell. Biomaterials 2006;27:5502.
[36] Dulinska I, Targosz M, Strojny W, Lekka M, Czuba P, Balwierz W, Szymonski M. Stiffness of normal and pathological erythrocytes studied by means of atomic force microscopy. J Biochem Biophys Methods 2006;66:1.
[37] Martin I, Quarto R, Dozin B, Cancedda R. Producing prefabricated tissues and organs via tissue engineering. IEEE Eng Med Biol Mag 1997;16:73.
[38] Ruoslahti E, Obrink B. Common principles in cell adhesion. Exp Cell Res 1996;227:1.
[39] Rosales C, O'Brien V, Kornberg L, Juliano R. Signal transduction by cell adhesion receptors. Biochim Biophys Acta 1995;1242:77.
[40] Critchley DR. Cytoskeletal proteins talin and vinculin in integrin-mediated adhesion. Biochem Soc Trans 2004;32:831.
[41] Tang DD, Anfinogenova Y. Physiologic properties and regulation of the actin cytoskeleton in vascular smooth muscle. J Cardiovasc Pharmacol Ther 2008;13:130.
[42] Chen GC, Turano B, Ruest PJ, Hagel M, Settleman J, Thomas SM. Regulation of Rho and Rac signaling to the actin cytoskeleton by paxillin during Drosophila development. Mol Cell Biol 2005;25:979.
[43] Ezzell RM, Goldmann WH, Wang N, Parashurama N, Ingber DE. Vinculin promotes cell spreading by mechanically coupling integrins to the cytoskeleton. Exp Cell Res 1997;231:14.
[44] Pelagalli A, Scibelli A, Lombardi P, d'Angelo D, Tortora G, Staiano N, Avallone L.

Expression of the focal adhesion protein paxillin in normal and breast cancer tissues. Vet Res Commun 2003;27 Suppl 1:343.
[45] Scibelli A, d'Angelo D, Pelagalli A, Tafuri S, Avallone L, Della Morte R, Staiano N. Expression levels of the focal adhesion-associated proteins paxillin and p130CAS in canine and feline mammary tumors. Vet Res 2003;34:193.
[46] Huang S, Ingber DE. Shape-dependent control of cell growth, differentiation, and apoptosis: switching between attractors in cell regulatory networks. Exp Cell Res 2000;261:91.
[47] Huang H, Sylvan J, Jonas M, Barresi R, So PT, Campbell KP, Lee RT. Cell stiffness and receptors: evidence for cytoskeletal subnetworks. Am J Physiol Cell Physiol 2005;288:C72.
[48] Kasza KE, Rowat AC, Liu J, Angelini TE, Brangwynne CP, Koenderink GH, Weitz DA. The cell as a material. Curr Opin Cell Biol 2007;19:101.
[49] Yamazaki D, Kurisu S, Takenawa T. Regulation of cancer cell motility through actin reorganization. Cancer Sci 2005;96:379.
[50] Rao KM, Cohen HJ. Actin cytoskeletal network in aging and cancer. Mutat Res 1991;256:139.
[51] Goldmann WH, Ezzell RM. Viscoelasticity in wild-type and vinculin-deficient (5.51) mouse F9 embryonic carcinoma cells examined by atomic force microscopy and rheology. Exp Cell Res 1996;226:234.
[52] Gallant ND, Michael KE, Garcia AJ. Cell adhesion strengthening: contributions of adhesive area, integrin binding, and focal adhesion assembly. Mol Biol Cell 2005;16:4329.
[53] Gallant ND, Garcia AJ. Model of integrin-mediated cell adhesion strengthening. J Biomech 2007;40:1301.
[54] Truskey GA, Proulx TL. Relationship between 3T3 cell spreading and the strength of adhesion on glass and silane surfaces. Biomaterials 1993;14:243.
[55] Groth T, Zlatanov I, Altankov G. Adhesion of human peripheral lymphocytes on biomaterials preadsorbed with fibronectin and vitronectin. J Biomater Sci Polym Ed 1994;6:729.
[56] Groth T, Altankov G, Klosz K. Adhesion of human peripheral blood lymphocytes is dependent on surface wettability and protein preadsorption. Biomaterials 1994;15:423.
[57] Uetsuka H, Onishi H, Henderson MA, White JM. Photoinduced redox reaction coupled with limited electron mobility at metal oxide surface. Journal of Physical Chemistry B 2004;108:10621.
[58] Henderson MA, White JM, Uetsuka H, Onishi H. Selectivity changes during organic photooxidation on TiO2: Role of O-2 pressure and organic coverage. Journal of Catalysis 2006;238:153.

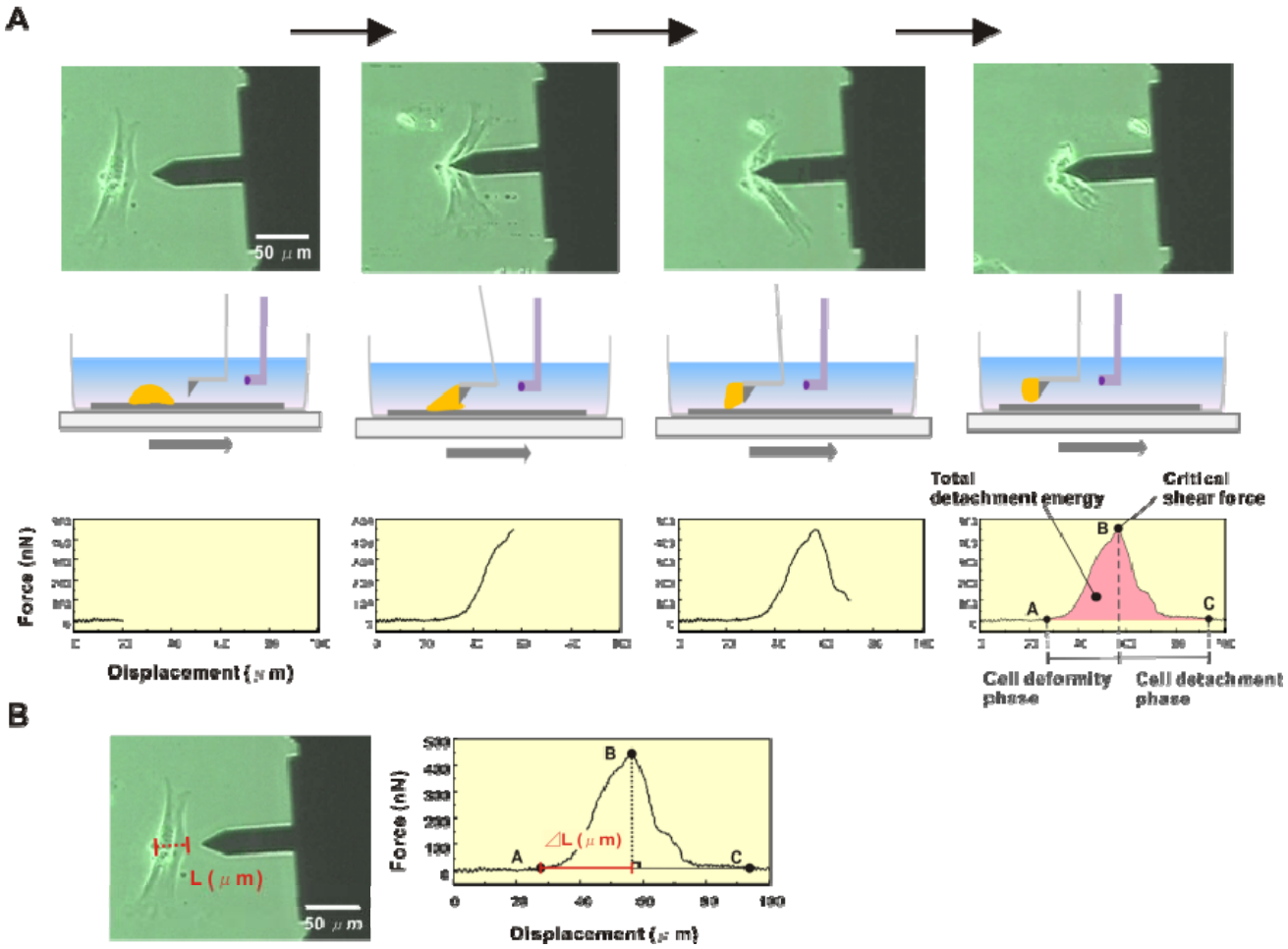
A
50 μm
Force (nN)
Displacement (μm)
Total detachment energy
Critical shear force
B
A
C
Cell deformity phase
Cell detachment phase
B
L (μm)
50 μm
Force (nN)
ΔL (μm)
A
B
C
Displacement (μm)

Figure 1

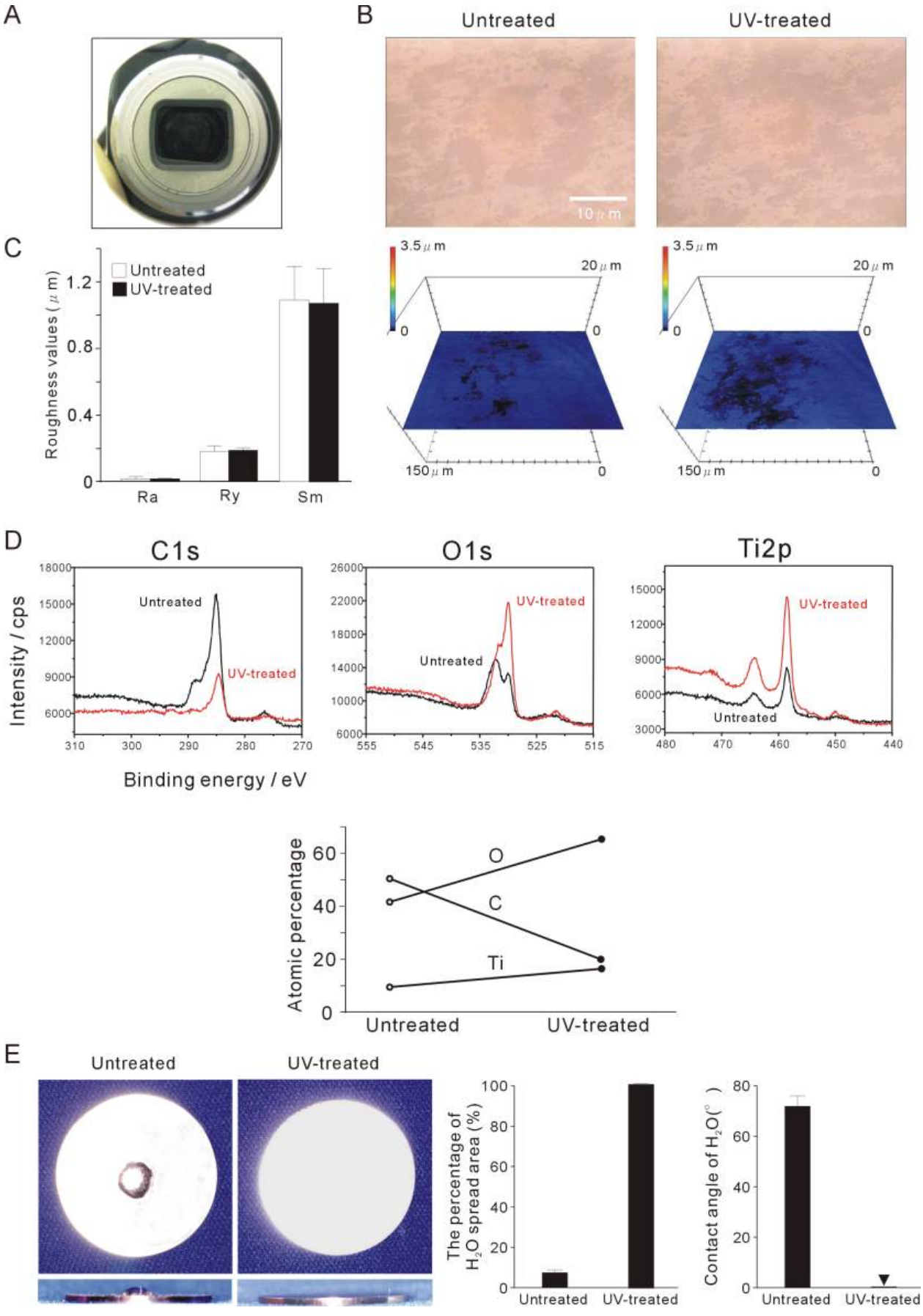
A
B
Untreated
UV-treated
10 μm
C
Untreated
UV-treated
Roughness values (μm)
1.2
0.8
0.4
0
Ra
Ry
Sm
3.5 μm
20 μm
0
150 μm
D
C1s
O1s
Ti2p
Intensity / cps
Binding energy / eV
Atomic percentage
60
40
20
O
C
Ti
E
The percentage of H2O spread area (%)
Contact angle of H2O(°)
100
80
60
40
20

Figure 2

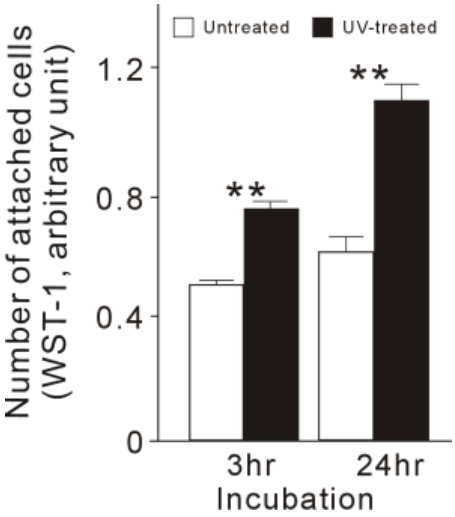
Untreated
UV-treated
Number of attached cells
(WST-1, arbitrary unit)
1.2
0.8
0.4
0
**
**
3hr
24hr
Incubation

Figure 3

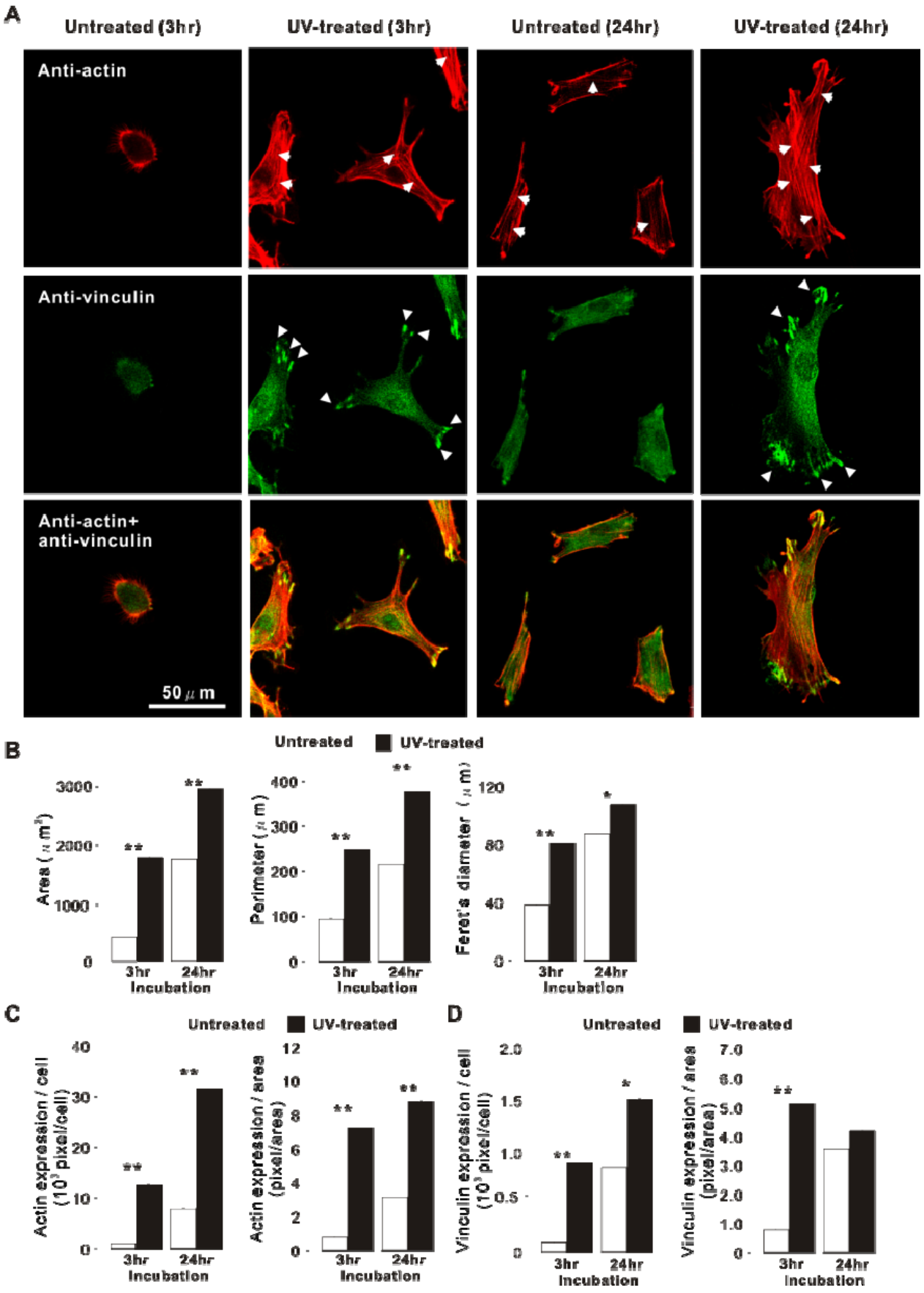
A
Untreated (3hr)
UV-treated (3hr)
Untreated (24hr)
UV-treated (24hr)
Anti-actin
Anti-vinculin
Anti-actin+
anti-vinculin
50 μm
B
Untreated
UV-treated
Area (μm²)
Perimeter (μm)
Feret's diameter (μm)
3hr
24hr
Incubation
C
Actin expression / cell (10³ pixel/cell)
Actin expression / area (pixel/area)
D
Vinculin expression / cell (10³ pixel/cell)
Vinculin expression / area (pixel/area)

Figure 4

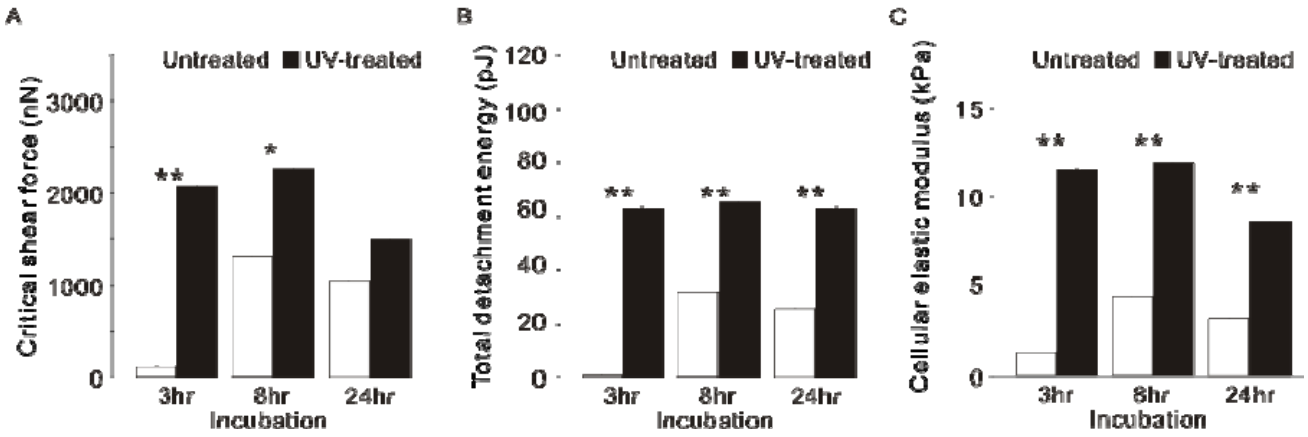
A
Untreated
UV-treated
Critical shear force (nN)
3000
2000
1000
0
**
*
3hr
8hr
24hr
Incubation
B
Untreated
UV-treated
Total detachment energy (pJ)
120
100
80
60
40
20
0
**
**
**
3hr
8hr
24hr
Incubation
C
Untreated
UV-treated
Cellular elastic modulus (kPa)
15
10
5
0
**
**
**
3hr
8hr
24hr
Incubation

Figure 5

Legends

Figure 1

Single-cell detachment technique used in this study to evaluate adhesive nature of single osteoblast on mirror-polished titanium surface. Technique is shear test-based and similar in principle to scratch test used in field of engineering and material sciences and atomic force microscopic technique. (A) Single-cell detachment is performed while monitoring under phase-contrast microscopy. Sequence of phase-contrast microscopic views of cell being pushed horizontally by tip of cantilever head (top row of images). Typical force-displacement curves obtained from single-cell detachment procedure and schematic descriptions of cell and pushing head in order of progression of shear test (left to right) corresponding to sequential microscopic images in top row of images are shown in middle and bottom rows, respectively. Parameters used in this study are described in rightmost panel. Point A is where tip of cantilever makes first contact with single cell, whereas Point B, where magnitude of pushing force reaches its peak, is assumed to be point where cell detachment is initiated. Subsequently, force applied starts to decrease until complete detachment of cell is attained (Point C). Until point B, no disruption of cell-material binding occurred, only deformation due to the load applied with the tip of the cantilever. After point B, cell detachment progresses, with disruption of each cell–material bond, one after the other. Force at Point B is defined as critical shear force, while area A-BC-A is supposed to correspond to total energy required to completely detach single cell and is, therefore, defined as total detachment energy. (B) Indication of cell width in moving direction of cantilever tip (L) and degree of displacement from initial contact of cantilever with cell (Point A) to critical shear force (Point B)(⊿L: distance between point A and D) are shown on left and right, respectively.

Figure 2

Surface characterization of a mirror-polished titanium surface and UV-induced alterations of its

physicochemical properties. (A) Macro-image of mirror-polished titanium surface. (B) High-magnification laser microscopic images (top) and 3-dimensional images (bottom) of mirror-polished titanium surfaces with or without UV-treatment. (C) Quantitative measurements of three surface roughness parameters (average roughness (Ra), peak-to-valley roughness (Ry) and inter irregularities space (Sm) for mirror-polished titanium surfaces with or without UV-treatment, based on laser microscopic analysis. Data represent mean ± SD (n = 3). (D) Intensity-binding energy profile and atomic percentage of carbon, oxygen and titanium on UV-treated or untreated mirror-polished titanium surfaces obtained from X-ray photoelectron spectroscopic (XPS) analysis. (E) Change in hydrophilic status of mirror-polished titanium surfaces with or without UV treatment. Photographic images of 10-μl H_2O droplets pipetted onto UV-treated or untreated mirror-polished titanium surfaces, as well as area of H_2O spread and contact angle of H_2O (histograms). Data represent mean ± SD (n = 3).

Figure 3

Initial bioactivity on mirror-polished titanium surfaces with or without UV treatment. Number of rat bone marrow-derived osteoblasts attached to UV-treated or untreated mirror-polished titanium surfaces at 3 or 24 hr incubation as evaluated by WST-1 colorimetric detection.

Figure 4

Initial spread, cytoskeletal arrangement and expression of focal adhesion protein vinculin in osteoblasts cultured on mirror-polished titanium surfaces with or without UV treatment. (A) Representative confocal microscopic images of cells stained with rhodamine phalloidin for actin filaments (red color, white arrowheads) and anti-vinculin (green color, white headings). Cells incubated on UV-treated or untreated TiO2 surfaces for 3 or 24 hr were used. (B) Cytomorphometric evaluations based on images presented in panel A. (C) Image analysis-based actin expression. Levels of actin expression per cell and per cell area were evaluated by densitometry using confocal

microscopic images presented in panel A. (D) Image analysis-based vinculin expressions per cell and per cell area. Data represent mean ± SD (n = 9) for panels B-D. *p < 0.05, **p < 0.01, indicating a statistically significant difference between UV-treated and untreated mirror-polished titanium surfaces (Bonferroni).

Figure 5

Cell adhesion strength and cellular mechanical properties of single osteoblast cultured on mirror-polished titanium surfaces with or without UV treatment. Critical shear force (A), total detachment energy (B) and cellular elastic modulus (C) of single osteoblast cultured on UV-treated or untreated mirror-polished titanium surfaces at after 3, 8 or 24 hr incubation. Data represent mean ± SD (n = 10) for all panels. *p < 0.05, **p < 0.01, indicating a statistically significant difference between UV-treated and untreated mirror-polished titanium surfaces (Bonferroni).